

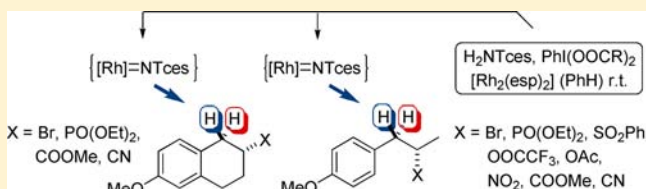
Diastereotopos-Differentiation in the Rh-Catalyzed Amination of Benzylic Methylene Groups in the α -Position to a Stereogenic Center

Anike Nörder, Sarah A. Warren, Eberhardt Herdtweck, Stefan M. Huber, and Thorsten Bach*

Department Chemie and Catalysis Research Center (CRC) Technische Universität München, D-85747 Garching, Germany

S Supporting Information

ABSTRACT: The diastereoselectivity of the Rh-catalyzed C–H amination was examined with 18 chiral open-chain substrates, which bear a benzylic methylene group in the α -position to a stereogenic center (–CHMeX), and with four chiral cyclic tetralins, in which the stereogenic center was positioned at carbon atom C2. The C–H amination was performed using trichloroethoxysulfonyl-substituted amine (H_2NTces) as the nitrogen source, a diacyloxyiodobenzene as the oxidant, and bis[rhodium($\alpha,\alpha,\alpha',\alpha'$ -tetramethyl-1,3-benzenedipropionate)] [$Rh_2(esp)_2$] as the catalyst. For acyclic substrates a high syn diastereoselectivity ($dr > 95/5$) was found if the substituent X was Br, PO(OEt) $_2$, SO $_2$ Ph, or OOCF $_3$ (eight examples). Moderate to good syn selectivities ($dr = 80/20$ to $91/9$) were found for X = NO $_2$, OAc, COOMe, and CN (eight examples). Only two substrates gave a low diastereoselectivity. Kinetic isotope effect (KIE) experiments revealed that there is no secondary KIE when replacing –CHMeCOOMe by –CDMeCOOMe, but there is a significant primary KIE at the benzylic methylene position (4.8 ± 0.7). Deuteration experiments provided evidence that the reaction proceeds stereospecifically with retention of configuration. A preferred conformation is proposed, which explains the outcome of the reaction. In this conformation the X substituent is antiperiplanar to the C–H bond, which is diastereoselectively attacked, and steric strain between the remaining substituents at the stereogenic and the prostereogenic center is minimized. DFT calculations support this model. They suggest, however, that the reaction is not concerted but occurs via hydrogen atom abstraction and subsequent radical rebound. Further support for an antiperiplanar attack relative to a given substituent X = Br, COOMe, or CN was obtained with the respective 2-substituted tetralins. Attack at C1 provides almost exclusively the trans-amination product. If the size of the X substituent increases [Br < CN < COOMe < PO(OEt) $_2$], attack at the carbon atom C4 prevails, delivering the respective trans-amination products at this position.



INTRODUCTION

Acyclic stereocontrol¹ has revolutionized the way organic chemists conceive and solve synthetic challenges in the total synthesis of complex natural products. For example, the prototypical question of facial diastereoselectivity in carbonyl addition reactions to α -chiral ketones or aldehydes² has been the source of literally hundreds of imaginative studies, which in turn have accumulated a wealth of information on the subject. There is a legion of diastereoselective substrate-induced reactions,³ and the number continues to grow to this date. Studies in this area have most commonly been concerned with the differentiation of diastereotopic faces at prostereogenic carbon atoms in double bonds. Less attention has been devoted to the differentiation of diastereotopic atoms or diastereotopic groups. Reactions, which occur with significant selectivity toward diastereotopic atoms or groups, are called diastereotopos-differentiating reactions.^{4,5} In connection with our interest in the facial diastereoselectivity of reactions at benzylic cation centers,⁶ we have some time ago performed some preliminary studies in the field of diastereotopos-differentiating C–H activation reactions.⁷ The key question was whether the two diastereotopic C–H bonds in benzylic substrates of type A (Figure 1) can be differentiated as a

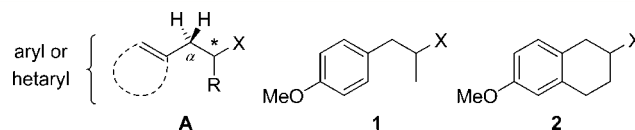


Figure 1. General structure of amination substrates A with the diastereotopic hydrogen atoms marked in α -position and more specific structures 1 and 2 of compounds used in the present study.

consequence of the steric and electronic properties of the substituents X, R, and H at the adjacent stereogenic center. As a test reaction the nitrene insertion (amination)^{8,9} of trichloroethoxysulfonyl-substituted amine (H_2NTces) with bis[rhodium($\alpha,\alpha,\alpha',\alpha'$ -tetramethyl-1,3-benzenedipropionate)] [$Rh_2(esp)_2$] as the catalyst and diacetoxyiodobenzene as the oxidant was chosen. This protocol has been successfully elaborated by Du Bois et al. and has shown its value for catalytic intermolecular amination reactions.¹⁰ No attempt was made on our part to improve the Du Bois protocol; rather, it served as a well-established test reaction to investigate the question of acyclic diastereotopos-differentiation.

Received: July 9, 2012

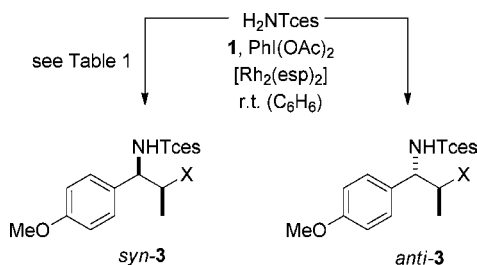
Published: August 6, 2012

It was found in preliminary work¹¹ that substrates **1** [X = PO(OEt)₂, SO₂Ph, NO₂, OAc, COOMe, CN] deliver an unexpectedly high diastereoselectivity in amination reactions and produce major diastereoisomers, in which the Tces-protected amino group resides *syn* to the methyl group in the representation chosen in Figure 1. The reaction was shown to proceed racemization-free if compounds of type **1** were used in enantiomerically pure form and therefore does hold some promise for diastereoselective C–H insertion reactions under acyclic stereocontrol. In order to collect further data about the effects, which are responsible for the diastereotopos-differentiation, additional studies have now been conducted with different precursors of general type **A**. In addition, DFT calculations have been performed, which support mechanistic conclusions drawn from the reaction of acyclic substrates **1** and of cyclic amination precursors **2**. Details of this work are reported in the present account.

RESULTS AND DISCUSSION

Acyclic Diastereotopos-Differentiation. Reactions with substrates **1** were performed in benzene solution using H₂NTces as the nitrogen source, PhI(OAc)₂ as the stoichiometric oxidant, and Rh₂(esp)₂ as the catalyst (Scheme 1). The diastereomeric products *syn*-**3** and *anti*-**3** were isolated

Scheme 1



as a mixture of diastereoisomers. Their relative ratio (dr) was determined by integration of appropriate signals in the ¹H NMR spectrum. It was shown that the diastereomeric ratio remained within an error limit of 5%, unchanged upon purification. However, a precise determination of the dr in the crude product mixture was difficult because unreacted substrate and reagents were still present. For better accuracy in the determination of the dr it was favorable to employ the purified mixture of diastereomers rather than the crude product mixture. It was ensured that the complete product was collected and that no change of the dr could occur. Indeed, most diastereoisomeric products showed identical R_f values. If this was not the case, the sample collection was followed by careful TLC analysis. When in doubt, the dr of the pure product mixtures was checked against the crude product.

The results of this comprehensive study are summarized in Table 1, in which the substrates are listed according to decreasing diastereoselectivity. The most selective reactions (dr > 95/5) were observed for heteroatomic substituents X = Br (entry 1), X = PO(OEt)₂ (entry 2), X = SO₂Ph (entry 3), and X = OOCF₃ (entry 4). The relative configuration of products *syn*-**3a**,¹² *syn*-**3b**, and *syn*-**3c** was determined by single crystal X-ray crystallography. The relative configuration of product *syn*-**3d** was assigned on the basis of analogy to the relative configuration determined by X-ray analysis for the major acetate diastereoisomer *syn*-**3f** (entry 6). To obtain unambig-

Table 1. Diastereotopos-Differentiation in C–H Amination Reactions at the Benzylic Position of Chiral Substrates **1**

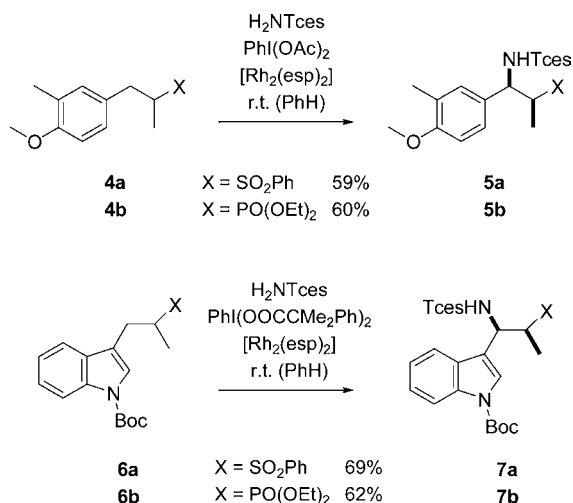
entry	substrate ^a	X	yield ^b [%]	dr ^c
1	1a	Br	89	>95/5
2	1b	PO(OEt) ₂	65	>95/5
3	1c	SO ₂ Ph	56	>95/5
4	1d	OOCF ₃	28 ^d	>95/5
5	1e	NO ₂	63	91/9
6	1f	OAc	40 ^d	86/14
7	1g	COOMe	81	82/18
8	1h	CN	86	80/20
9	1i	CH ₂ OTBS	44	62/38
10	1j	CH ₂ OAc	70	60/40

^aH₂NTces (0.5 mmol) and Rh₂(esp)₂ (0.01 mmol) were dissolved in benzene (1.5 mL). Substrate **1** (1.0 mmol) was added to the stirred solution at 25 °C, and the oxidant (0.75 mmol) was added in portions over 2 h. The reaction was quenched with a saturated aqueous solution of thiourea (5 mL) after 16 h. ^bYields of the diastereomeric mixture based on nitrene source H₂NTces. ^cThe diastereomeric ratio (dr = *syn*/*anti*) was determined by ¹H NMR. ^dIncomplete conversion; impure H₂NTces was reisolated.

uous evidence, the major product *syn*-**3d** was converted into acetate *syn*-**3f** by reduction (NaBH₄ in MeOH)¹³ to the free alcohol and subsequent acetylation (Ac₂O, DMAP, NEt₃).¹⁴ Acetate **1f** belongs together with nitro compound **1e** (entry 5), ester **1g** (entry 7), and nitrile **1h** (entry 8) to the substrates, which gave moderate to good selectivities (dr = 80/20 to 91/9). While the relative configuration of products *syn*-**3e** and *syn*-**3g** were also proven by X-ray analysis,¹¹ the configuration of nitrile *syn*-**3h** was elucidated by its conversion into methyl ester *syn*-**3g** employing the Pinner reaction¹⁵ (HCl in MeOH). The protected primary alcohol derivatives **1i** (entry 9) and **1j** (entry 10) exhibited only low diastereoselectivity, and no effort was made to determine the relative configuration of the major diastereoisomer. However, on the bases of analogy and mechanistic considerations (vide infra) it appears likely that the major diastereoisomer was the *syn* product. In general, no H₂NTces was recovered in the amination reaction, and the reaction was complete regarding its conversion. Only in two cases (entries 4 and 6) was it apparent that the reaction had not gone to completion. Since the separation of H₂NTces from the products was difficult, the amount of recovered H₂NTces could not be quantified, and the relative low yields in these cases were due to incomplete conversion and separation problems. The yields provided in Table 1 refer to pure products **3** and are not based on recovered starting material.

Electronic and steric factors regarding the substituent X limited the scope of the study in a few directions. For large groups X (X = *t*-Bu, CMe₂OAc) there were only traces of product detectable, and the nitrogen source was largely reisolated. If the substituent X was an oxygen substituent, which was *not* acceptor substituted, e.g. X = OH, OMe, OTMS, there was no conversion at all. From a synthetic point of view the results, in which a single diastereoisomer was the exclusive product, are certainly most useful. A few substrates related to phosphonate **1b** and sulfone **1c** were synthesized and submitted to the amination conditions (Scheme 2). It turned out that the reactions proceeded equally selective for precursors **4** and **6**, giving stereoselective access to β-amino substituted phosphonates and sulfones **5** and **7**. Diastereomerically pure (dr > 95/5) products were isolated, to which the *syn* configuration was assigned on the basis of analogy. The

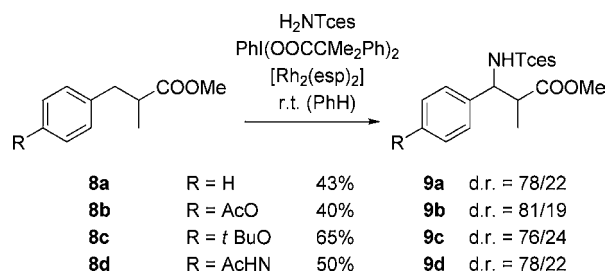
Scheme 2



functional group tolerance of the amination conditions toward the indole core and the *tert*-butoxycarbonyl (Boc) group is notable. Despite the fact that synthetic optimization of the amination reaction was not the focus of this work, the finding by Du Bois et al.,¹⁶ that $\text{PhI}(\text{OOCMe}_2\text{Ph})_2$ is in many cases an oxidant superior to diacetoxyiodobenzene, could be corroborated. Yields in the reaction of indole derivatives **5** were significantly higher with the former oxidation reagent than with the latter.

By choosing substrates **8** with a moderately strong directing group X (X = COOMe) at the stereogenic center, it was explored whether the para substituent R in the benzylic substrate exerts a significant influence on the diastereoselectivity (Scheme 3). For this study, $\text{PhI}(\text{OOCMe}_2\text{Ph})_2$ turned out

Scheme 3



to be the superior oxidant. In the case of *N*-acetylaniline **8d** the oxidant was added by syringe pump. In all other cases it was added over 2 h in portions. The diastereoselectivity of the reactions varied little as compared to those of the reaction of the *p*-methoxy-substituted substrate **1g** (Table 1, entry 7, dr = 82/18), and a significant influence of R was not detected. The reactivity of the substrates was sufficient, and products **9** were obtained in good to moderate yields (40–65%). If the substituent R was strongly electron withdrawing (R = NO_2), no amination reaction was observed. The latter observation is in accord with the electrophilic nature of the putative rhodium nitrenoid intermediate (*vide infra*).

The stereochemical outcome was not dependent on the choice of the amine protecting group. Reactions performed with *p*-nitrobenzenesulfonyl-protected amine (NsNH_2)¹⁷ under otherwise identical conditions resulted in the same diastereoselectivity. As an example, conversion of bromide **1a**

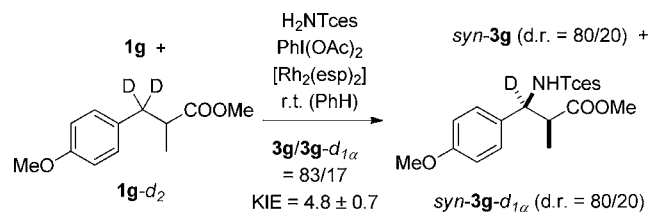
gave the respective C–H amination product in 59% yield and with a dr > 95/5 (see SI for further details).

Reaction of Deuterated Substrates. Two deuterated substrates **1g-d₁** (Scheme 4) and **1g-d₂** (Scheme 5) were

Scheme 4



Scheme 5



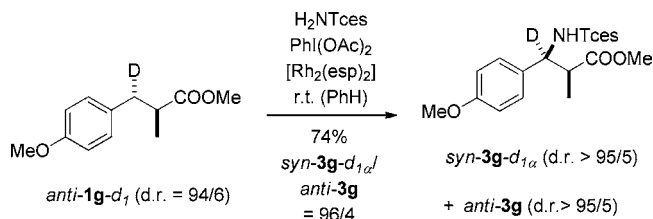
prepared in order to obtain possible information about the reaction course via kinetic isotope effects (KIEs). In the first experiment, ester **1g-d₁**, which was readily available by quantitative deuteration of ester **1g** and subsequent quench with D_2O , was subjected to the amination reaction conditions in an intermolecular competition experiment with the undeuterated substrate **1g**. No secondary KIE was observed (Scheme 4). The products **3g** and **3g-d₁** were obtained in a 50/50 ratio at the detection level of ^1H NMR spectroscopy. The predominant product was the *syn* product, **syn-3g-d₁**, and there were no differences in the diastereomeric ratio compared to that of the undeuterated product **syn-3g**.

A second experiment was performed with a doubly deuterated substrate **1g-d₂**, which carried both deuterium atoms in the benzylic position. The substrate was readily available by alkylation of methyl propionate with *p*-methoxybenzyl bromide- d_2 (see Supporting Information). In the amination experiments a significant primary KIE was detected. The deuterated substrate, **1g-d₂**, reacted significantly more slowly than the undeuterated substrate, **1g** (Scheme 5). The diastereomeric ratio remained unchanged, and the α -monodeuterated product **3g-d_{1α}** was formed also predominantly as the *syn*-diastereoisomer.

Deuterated substrates were also employed to address the question of stereospecificity in the amination reaction. The monodeuterated compounds **syn-1g-d₁** and **anti-1g-d₁** were obtained by reduction of the respective alcohols with Et_3SiH or Et_3SiD (see Supporting Information), which occurs with high diastereoselectivity (dr = 94/6) via chiral benzylic carbocations.⁶ If the amination proceeds with retention of configuration, it is expected that the amination provides a maximum of two products. Given the preference for hydrogen abstraction over deuterium abstraction (KIE = 4.8) and given the observed diastereoselectivity in the amination of substrate **1g** (dr = 82/18), it was anticipated that substrate **anti-1g-d₁** would provide essentially a single product, in what could be considered a matched situation. Indeed, product **syn-3g-d_{1α}** was observed as

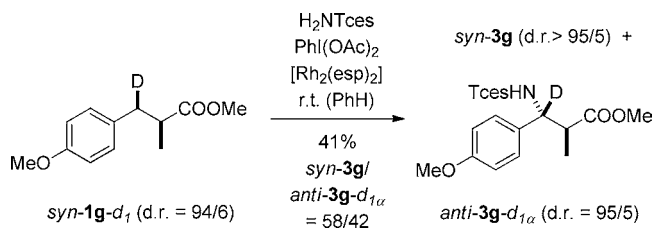
the predominant product together with minor amounts (4%) of *anti*-**3g** (Scheme 6).

Scheme 6



In the mismatched situation expected for substrate *syn*-**1g**-*d*₁ and under the provision that the reaction proceeds stereospecifically, two products should be formed in almost equal amounts. Indeed, when submitting substrate *syn*-**1g**-*d*₁ to the typical reaction conditions of the amination reaction (Table 1) we observed a relatively slow reaction, which led to two products, i.e. the nondeuterated product *syn*-**3g** (dr > 95/5) and the deuterated product *anti*-**3g**-*d*_{1 α} (dr = 95/5). The product ratio was 58/42 (Scheme 7).

Scheme 7



The latter study provides unambiguous evidence that the amination at the benzylic methylene group of substrates **1** proceeds stereospecifically with retention of configuration. This result is in line with previously reported experiments performed at tertiary benzylic C–H bonds, which was also shown to occur stereospecifically.^{10b}

Mechanistic Considerations and DFT Calculations. It is generally accepted that Rh-catalyzed nitrene insertion reactions proceed via an intermediate Rh nitrene complex, in which the nitrene is bound to the free coordination site of the binuclear Rh complex. In analogy to the Rh-catalyzed carbene insertion reaction the insertion of a rhodium nitrenoid into a C–H bond has been described to occur in a “concerted but highly asynchronous manner” (concerted mechanism).^{18,19} Alternatively, the reaction pathway can be envisaged to include a complete hydrogen abstraction by the nitrenoid complex and a subsequent rapid C–N bond formation (rebound mechanism).²⁰ In either case, the electrophilic nitrogen atom pulls off the hydrogen atom from the carbon atom, to which the latter is bound. An incipient positive charge develops at the carbon atom, and the nitrogen atom becomes negatively charged. When considering possible staggered conformations **I**–**III** of substrates **1** (Figure 2), it is obvious that C–H insertion into the carbon–hydrogen bond marked by a red box provides the *anti* products *anti*-**3**, whereas C–H insertion into the carbon–hydrogen bond marked in blue gives the *syn* products *syn*-**3**.

Upon its way to the transition state the hydrogen atom becomes detached from the prostereogenic carbon center. On the basis of the fact that the carbon atom, to which the nitrogen

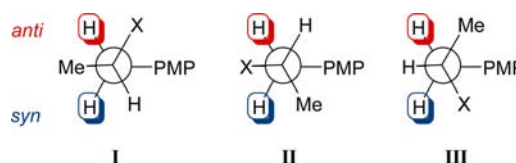


Figure 2. Conformations **I**–**III** responsible for the formation of either *anti* or *syn* diastereomeric products in the reaction of substrates **1** (PMP = *p*-methoxyphenyl).

substituent is eventually attached, has positive partial charge in the transition state of the amination reactions, we had earlier considered¹¹ conformation **II** to be responsible for the diastereoselection, because we speculated that the incipient positive charge would be best stabilized by an antiperiplanar C–H bond. As a result, the favored transition state should be transition state $\text{TS}_{\text{syn-II}}$ (Figure 3), which emanates from

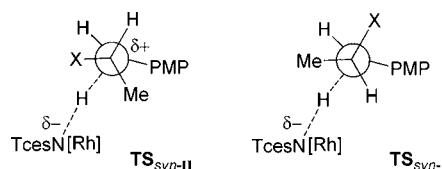


Figure 3. Transition states $\text{TS}_{\text{syn-II}}$ and $\text{TS}_{\text{syn-I}}$ of a diastereoselective amination reaction evolving from two of the conformations depicted in Figure 2.

conformation **II** and in which the *syn* hydrogen atom is abstracted. In this graphic, [Rh] symbolizes a ligated rhodium metal center. The question whether the reaction proceeds stepwise or concerted is not relevant to this discussion but will be addressed further below. A normal (positive) secondary KIE was expected if such a hyperconjugative stabilization was significant. In the reaction of **1g**-*d*₁ (Scheme 4) no KIE was detectable ($k_{\text{H}}/k_{\text{D}} = 1.0$), however, and there was no change in diastereoselectivity when comparing the respective products, **3g** and **3g**-*d*₁. Although it is well established that secondary kinetic deuterium isotope effects are not high,²¹ the results raised doubts about the initial hypothesis. This was more true as it was not clear why conformation *syn*-**II** would be different from conformation *anti*-**I** (Figure 2) with an antiperiplanar C–H bond to the “wrong” hydrogen atom (*anti*-H). In addition, the repulsion of the substituent X with the partially negative charge at the reactive nitrogen atom was not taken into account. This interaction would be minimized in conformations **I** (for *syn*-H) via $\text{TS}_{\text{syn-I}}$ (Figure 3) and **III** (for *anti*-H).

In order to obtain a more detailed picture about the C–H insertion reaction, DFT calculations were performed. A related theoretical study on the intramolecular amidation of carbamates by Che et al.²² came to the conclusion that $\text{Rh}_2^{\text{II,II}}$ -nitrene complexes are the actual NR-delivering intermediates, with the respective triplet species being slightly more favorable than the singlet species. Two feasible reaction pathways were investigated: namely, a concerted insertion mechanism by a singlet nitrenoid and a radical abstraction/recombination pathway by a triplet nitrenoid. Che et al. found the singlet reaction pathway to be more favorable overall for the intramolecular transformation they studied. Since the findings of Che et al.²² were in accord with experimental results by Espino and Du Bois,²³ we chose to employ the same computational method for our investigations, i.e. the Becke BPW91 functional²⁴ with a 6-31G* basis set for all atoms except Rh, for which the LANL2DZ²⁵

basis set with the corresponding pseudopotential was used (for more details see the Supporting Information). For computational efficiency, the *p*-methoxyphenyl substituent and the acetate ligands were replaced by a phenyl substituent and formate ligands, respectively. The nitro group was chosen as a prototypical X substituent, and for all possible conformations of the substrate (denoted I to III in analogy to Figure 2), the corresponding transition states for the reaction with the $\text{Rh}_2^{\text{II,II}}$ -nitrene complex were determined.

Despite various attempts to find concerted transition states on the singlet energy surface, no such species could be obtained. Instead, singlet transition states corresponding to a hydride transfer from the substrate to the nitrogen atom of the nitrene species were found. Thus, in stark contrast to the findings by Che et al. for an *intramolecular* transformation (see above), the *intermolecular* reaction considered here seems to proceed on the singlet surface via a hydrogen atom transfer/recombination pathway. The most favorable of the singlet transition states, however, corresponding to the reaction of *syn*-I with the nitrenoid, was less favorable by about 9.5 kJ/mol in free energy than the most favorable triplet transition state ($\text{TS}_{\text{syn-I}}$ see below).

On the triplet energy surface, transition states for the hydrogen atom abstraction by the nitrenoid were determined for all six reactive orientations of the substrate (compare Figure 2).²⁶ As already indicated, the most favorable transition state was the one referring to *syn*-I, analogous to the singlet case. This transition state, $\text{TS}_{\text{syn-I}}$ (Figure 4) features the lowest

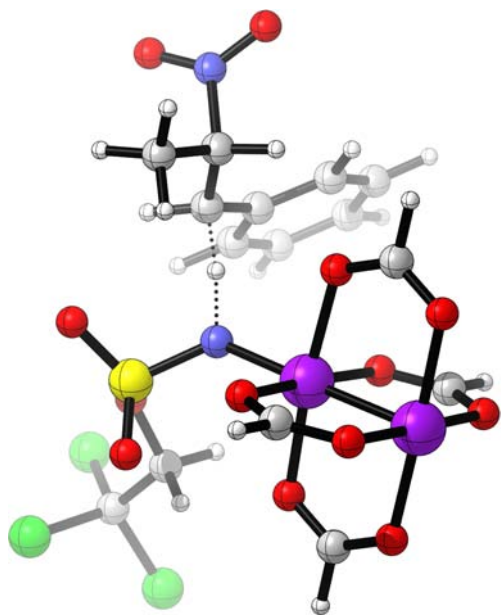


Figure 4. Most favorable (triplet) transition state $\text{TS}_{\text{syn-I}}$. Purple = Rh, yellow = S, green = Cl, blue = N, red = O, gray = C, white = H. The figure was prepared with CYLview.²⁷

relative free energy with respect to the other alternatives, as well as the lowest activation barrier of all six hydrogen abstraction processes (58 kJ/mol). More precisely, the transition states corresponding to the abstraction of the anti hydrogen atom of the substrate (as denoted in Figure 2) are approximately 39 kJ/mol ($\text{TS}_{\text{anti-I}}$), 9 kJ/mol ($\text{TS}_{\text{anti-II}}$), and 14 kJ/mol ($\text{TS}_{\text{anti-III}}$) higher in energy and feature activation barriers of at least 67 kJ/mol ($\text{TS}_{\text{anti-III}}$).

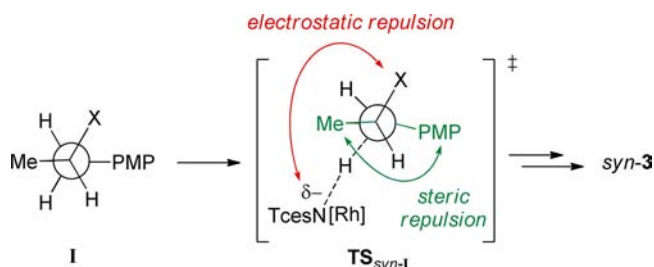
The two alternative transition states for the abstraction of the *syn* hydrogen of the substrate (Figure 2) are 47 kJ/mol ($\text{TS}_{\text{syn-II}}$) and 16 kJ/mol ($\text{TS}_{\text{syn-III}}$) higher in free energy and feature activation barriers of at least 69 kJ/mol ($\text{TS}_{\text{syn-III}}$). The most favorable transition state $\text{TS}_{\text{syn-I}}$ shown in Figure 4, explains the experimental findings presented above (Table 1, substrate **1e**), assuming that the two radicals formed in the hydrogen abstraction step quickly recombine in a subsequent step. In $\text{TS}_{\text{syn-I}}$ the hydrogen abstraction proceeds via a quasi-linear arrangement of C–H–N (173°), with a C–H distance of 1.30 Å (vs 1.10 Å in the isolated substrate) and a H–N distance of 1.40 Å. Other notable differences in geometrical features of the transition state compared to those of the starting materials include a somewhat narrower Rh–N–S angle within the nitrenoid part (128° vs 133° in the isolated nitrenoid) and a C–C bond of the carbon at the hydrogen abstraction site that is shortened with respect to that in the phenyl moiety (1.47 Å vs 1.52 Å in the isolated substrate). In addition, the sum of angles of the three unreactive bonds around the carbon atom of the hydrogen abstraction site indicate that the substrate is already markedly planarized (345° vs 333° in the isolated substrate and 360° in the radical). Mulliken atomic spin densities show that the spin is mainly located at the nitrogen of the nitrenoid (0.70) and the carbon of the hydrogen abstraction site (0.30), whereas the hydrogen atom itself carries only negligible spin density (-0.02).

Further insight into the nature of the transition state was sought by an analysis of the charge densities, obtained by a natural bond order (NBO)²⁸ analysis. Analogous to the situation discussed above for the concerted singlet mechanism, the nitrogen atom of the nitrenoid is markedly more negatively charged (-0.73 vs -0.52 in the isolated nitrenoid), while the carbon atom of the abstraction site and the hydrogen atom itself are somewhat more positively charged (-0.42 vs -0.51 and $+0.34$ vs $+0.26$ in the transition state vs the pure substrate, respectively). Overall, the substrate fragment without the leaving hydrogen atom is almost neutral in the transition state (overall charge $+0.01$), while the nitrenoid part features a negative charge that is essentially equivalent (in absolute terms) to the positive charge of the hydrogen atom (-0.35 vs $+0.34$).

The energetic preference of $\text{TS}_{\text{syn-I}}$ over the five alternative transition states is likely based on steric and electronic reasons. For instance, in the transition states $\text{TS}_{\text{anti-I}}$ and $\text{TS}_{\text{syn-II}}$, both the X (nitro) and the methyl substituent of the saturated carbon atom next to the hydrogen abstraction site point toward the nitrenoid, likely causing increased steric hindrance in comparison with the four remaining alternative transition states, which feature at least one hydrogen atom pointing toward the nitrenoid instead. In the fragment $-\text{CHMeNO}_2$ the nitro group bears a significant negative charge (-0.20). It is therefore likely that the electrostatic repulsion between the nitro group and the nitrogen atom of the nitrenoid force the nitro group to adopt a conformation that is antiperiplanar to the abstracted hydrogen atom (Scheme 8).

The same argument holds for all other substituents X, which should encounter a similar repulsion. In order to get an idea whether additional electronic effects might stabilize $\text{TS}_{\text{syn-I}}$ we took the geometries of the substrate part of the transition states (without the leaving hydrogen atom) and determined the relative stabilities of the respective radical species (i.e., without reoptimizing the geometry). Indeed, the radical corresponding to $\text{TS}_{\text{syn-I}}$ was significantly more stable than the ones referring to the other transition states (with the next most stable ones,

Scheme 8



corresponding to $TS_{anti-II}$ and $TS_{anti-IV}$ being respectively 4 and 9 kJ/mol less stable).

The primary KIE for a reaction via transition state TS_{syn-I} was estimated computationally by replacing the abstracted hydrogen atom by a deuterium atom. The obtained value was approximately 5.7 (see Supporting Information), which is slightly higher than the experimental value (Scheme 5). However, it should be noted that primary KIEs between 3.5 and 5.0²⁹ have been reported^{19c,g,20b} for related Rh-catalyzed amination reactions, for which the authors postulated a concerted mechanism.

Cyclic Diastereotopos-Differentiation. Previous results and the DFT calculations indicated that the diastereotopos-differentiation might be due to a preferred C–H amination anti to a given substituent X. In a cyclic array, a distinction between an anti or syn approach relative to a given substituent is easily possible. In substrates **2** for example the α -hydrogen atom at position C1 of the tetralin is anti to the substituent X, whereas the β -hydrogen atom is in a syn relationship (Figure 5). It

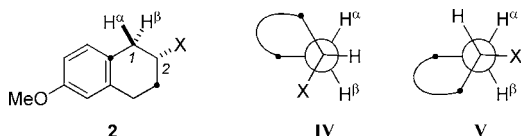
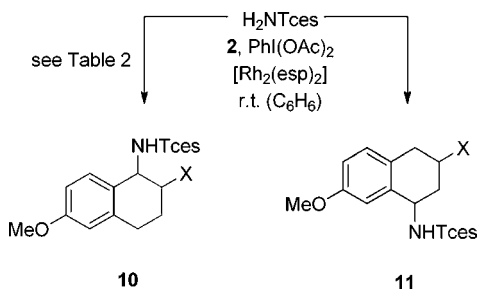


Figure 5. Chiral tetralin substrates **2** with two diastereotopic hydrogen atoms H^α and H^β and possible conformations **IV** and **V**.

should be possible for the substrates to adopt conformation **IV** and **V**, in which either the substituent X or the hydrogen atom at C2 is antiperiplanar to the adjacent hydrogen atom at C1. If the above-mentioned hypothesis was correct, a significant preference for amination at the α -hydrogen atom was to be observed leading to a *trans*-1,2-disubstituted tetralin.

Reactions with substrates **2** were performed under the conditions previously employed for the reaction of acyclic substrates **1**. The chemoselectivity of the amination was satisfactory (Scheme 9, Table 2), and yields were in the

Scheme 9



range of 60–70% for all four cases studied. However, it was found that the regioselectivity of the attack varied, depending on the substituent X. For X = Br (entry 1) the expected C1-amination product **10a** was exclusively formed, whereas all other substrates (entries 2–4) gave product mixtures, in which both C1- and C4-amination products could be detected. Although the purpose of these experiments was to study the diastereoselectivity of the amination reaction at C1 (products **10**), the observation of C4-amination products **11** is interesting and will be discussed further below. Regarding the diastereoselectivity at C1, it is notable that in all four cases a high selectivity was observed for the formation of one diastereoisomer (dr = 90/10 to >95/5).

The structure elucidation of products **10** (Figure 6) could only be performed for products **10a**, **10c**, and **10d**. The reaction of phosphonate **2b** resulted in insufficient quantities of product **10b**, which in addition was difficult to separate from other diastereo- and regioisomers. The relative configuration of product **10d** was unequivocally established by single-crystal X-ray analysis as *trans* (*trans*-**10d**).³⁰ A remarkable feature of the product conformation, which was further corroborated by NMR data, is the perfectly antiperiplanar position of the cyano group at C2 and the NHTces group at C1. The coupling constant for the protons at C1 and C2 is low ($^3J = 3.3$ Hz) indicating that this conformation is also prevalent in solution. The relative configuration of bromide **10a** was elucidated by comparison with compound *trans*-**10a**, which was independently prepared by the stereospecific anti-aminobromination³¹ of the respective 3,4-dihydronaphthalene (see SI for further details). The major diastereomeric C–H amination product obtained from substrate **2a** was in all respects identical to this compound. As observed for *trans*-**10d**, the low coupling constant for the protons at C1 and C2 ($^3J = 2.7$ Hz) indicates a preferred antiperiplanar orientation of the two substituents at C1 and C2. The *trans*-configuration was also assigned to the major diastereoisomer obtained by C–H amination of ester **2c**. In this case the compound was independently synthesized from diastereomerically pure nitrile *trans*-**10d** by a Pinner reaction. Despite the fact that the Pinner reaction did not proceed in high yields (see SI), the identity of the compounds could be clearly established by ¹H NMR spectroscopy. The coupling constant for the protons at C1 and C2 is $^3J = 4.9$ Hz.

From the results with substrates **2a**, **2c**, and **2d** it is clear that C–H insertion occurs at C1 selectively at the α -hydrogen atom leading to the respective *trans* products. It is very likely that the reaction proceeds via conformation **IV** (Figure 5), in which the X substituent adopts an axial position and in which the axial hydrogen atom is attacked. This conformation gets more disfavored the larger the X substituent becomes. There is apparently no reaction at C1 via conformation **V** with an equatorial X substituent and an axial hydrogen atom at C2. Instead of a reaction at C1 the respective amination takes place at the C4–H bond. In line with a previous result^{10b} the respective attack leads to *trans*-configured products. For methyl ester **11c** and cyanide **11d**, the configuration of the major diastereoisomers was elucidated by single-crystal X-ray analysis and the relative configuration confirmed to be *trans*-**11c**³² and *trans*-**11d**.³³ In the products, the substituents X are located equatorially, and the NHTces is in an axial position. Like the *trans* products, *trans*-**10**, the *trans* products at C4 are likely to result also from an amination at the axial C–H bond.

Table 2. Regio- and Diastereoselectivity in C–H Amination Reactions at the Benzylic Position of Chiral Tetralin Substrates 2

entry	substrate ^a	X	yield ^b [%]	rr ^c	dr ^d (10)	dr ^e (11)
1	2a	Br	80	>95/5	>95/5	—
2	2b	PO(OEt) ₂	58	20/80	90/10	>95/5
3	2c	COOMe	68	57/43	95/5	88/12
4	2d	CN	66	83/17	95/5	80/20

^aH₂NTces (0.5 mmol) and Rh₂(esp)₂ (0.01 mmol) were dissolved in benzene (1.5 mL). Substrate 2 (1.0 mmol) was added to the stirred solution at 25 °C, and the oxidant (0.75 mmol) was added in portions over 2 h. The reaction was quenched with a saturated aqueous solution of thiourea (5 mL) after 16 h. ^bYields of the product mixture based on nitrene source H₂NTces. ^cThe regioisomeric ratio (rr = 10/11) was determined by ¹H NMR. ^dThe diastereomeric ratio (dr = trans/cis) of compounds 10 was determined by ¹H NMR. ^eThe diastereomeric ratio (dr = trans/cis) of compounds 11 was determined by ¹H NMR.

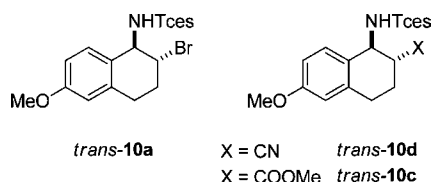


Figure 6. Products *trans*-10a, *trans*-10c, and *trans*-10d obtained by diastereoselective C–H amination of tetralins.

CONCLUSION

In summary, the experiments performed with acyclic substrates 1 and with cyclic substrates 2 provide, in combination with the DFT calculations, a reasonable model for the selectivity-determining step in the diastereoselective C–H amination of methylene groups. The intermolecular approach of the rhodium nitrenoid to a given C–H bond occurs antiperiplanar to heteroatom substituents (X = Br, PO(OEt)₂, SO₂Ph, OOCF₃, NO₂, OAc) or electron-withdrawing groups (X = COOMe, CN). The electrostatic repulsion between these substituents and the incipient negative charge at the nitrene nitrogen atom is likely the reason for the conformational preference. In acyclic substrates, this preference leads to the predominant formation of *syn* products *syn*-3, which can be synthetically useful as shown for several cases (e.g., products 5 and 7). In cyclic substrates, only axially positioned C–H bonds are attacked, which leads in 2-substituted tetralins to C1 amination only if the substituents X can adopt an axial position (X = Br, CN, COOMe). A high selectivity in favor of the *trans* products is observed. For larger substituents [X = PO(OEt)₂], which reside in an equatorial position, the selective axial attack at C4 prevails. In contrast to previous calculations on intramolecular C–H amination reactions, our DFT calculations suggest the intermolecular C–H amination reaction to be nonconcerted. Rather, C–H abstraction precedes a subsequent C–N bond formation.

ASSOCIATED CONTENT

Supporting Information

Detailed experimental procedures, characterization data for new compounds, X-ray crystallographic data, and details of the DFT calculations. This material is available free of charge via the Internet at <http://pubs.acs.org>.

AUTHOR INFORMATION

Corresponding Author

thorsten.bach@ch.tum.de

Notes

The authors declare no competing financial interest.

ACKNOWLEDGMENTS

This project was supported by the *Deutsche Forschungsgemeinschaft* (Ba 1372-12) and by the *TUM Graduate School*. S.M.H. acknowledges the *Fonds der Chemischen Industrie* for a Liebig fellowship. We thank Dr. Markus Drees (TU München) for helpful discussions regarding the computation of KIEs.

REFERENCES

- (1) (a) O'Brien, A. G. *Tetrahedron* **2011**, *67*, 9639–9667. (b) Heathcock, C. H. *Science* **1981**, *214*, 395–400. (c) Bartlett, P. A. *Tetrahedron* **1980**, *36*, 2–72.
- (2) Review: Mengel, A.; Reiser, O. *Chem. Rev.* **1999**, *99*, 1191–1223.
- (3) (a) Nógrádi, M. *Stereoselective Synthesis*, 2nd ed.; VCH: Weinheim, 1995. (b) Helmchen, G.; Hoffmann, R. W.; Mulzer, J.; Schaumann, E., Eds. In *Houben Weyl: Methods of Organic Chemistry*; Thieme: Stuttgart, 1996; Vol. E21. (c) Carreira, E. M.; Kyaemo, L. *Classics in Stereoselective Synthesis*; VCH: Weinheim, 2008. (d) de Vries, J. G.; Molander, G. A.; Evans, P. A., Eds. *Stereoselective Synthesis*; Thieme: Stuttgart, 2011; Vols. 1–3.
- (4) For the definition, see: Izumi, Y.; Tai, A. *Stereo-differentiating Reactions*; Academic Press: New York, 1977.
- (5) General review on diastereotopos-differentiating reactions: Hoffmann, R. W. *Synthesis* **2004**, 2075–2090.
- (6) (a) Mühlthau, F.; Schuster, O.; Bach, T. *J. Am. Chem. Soc.* **2005**, *127*, 9348–9349. (b) Mühlthau, F.; Stadler, D.; Goepfert, A.; Olah, G. A.; Prakash, G. K. S.; Bach, T. *J. Am. Chem. Soc.* **2006**, *128*, 9668–9675. (c) Stadler, D.; Mühlthau, F.; Rubenbauer, P.; Herdtweck, E.; Bach, T. *Synlett* **2006**, 2573–2576. (d) Stadler, D.; Bach, T. *Chem.—Asian J.* **2008**, *3*, 272–284. (e) Stadler, D.; Goepfert, A.; Rasul, G.; Olah, G. A.; Prakash, G. K. S.; Bach, T. *J. Org. Chem.* **2009**, *74*, 312–318.
- (7) Review: Herrmann, P.; Bach, T. *Chem. Soc. Rev.* **2011**, *40*, 2022–2038.
- (8) Recent reviews: (a) Collet, F.; Lescot, C.; Dauban, P. *Chem. Soc. Rev.* **2011**, *40*, 1926–1936. (b) Du Bois, J. *Org. Process Res. Dev.* **2011**, *15*, 758–762. (c) Zalatan, D. N.; Du Bois, J. *Top. Curr. Chem.* **2010**, *292*, 347–378. (d) Collet, F.; Dodd, R. H.; Dauban, P. *Chem. Commun.* **2009**, 5061–5074. (e) Müller, P.; Fruit, C. *Chem. Rev.* **2003**, *103*, 2905–2920.
- (9) For recent contributions to intermolecular C–H amination reactions, see: (a) Lebel, H.; Spitz, C.; Leogane, O.; Trudel, C.; Parmentier, M. *Org. Lett.* **2011**, *13*, 5460–5463. (b) Lu, H.; Subbarayan, V.; Tao, J.; Zhang, X. P. *Organometallics* **2010**, *29*, 389–393. (c) Collet, F.; Lescot, C.; Liang, C.; Dauban, P. *Dalton Trans.* **2010**, 39, 10401–10413. (d) Fan, R.; Li, W.; Pu, D.; Zhang, L. *Org. Lett.* **2009**, *11*, 1425–1428. (e) Liang, C.; Collet, F.; Robert-Peillard, F.; Müller, P.; Dodd, R. H.; Dauban, P. *J. Am. Chem. Soc.* **2008**, *130*, 343–350. (f) Badié, Y. M.; Dinescu, A.; Dai, X.; Palomino, R. M.; Heinemann, F. W.; Cundari, T. R.; Warren, T. H. *Angew. Chem., Int. Ed.* **2008**, *47*, 9961–9964. (g) Huard, K.; Lebel, H. *Chem.—Eur. J.* **2008**, *14*, 6222–6230.
- (10) Key references: (a) Espino, C. G.; Fiori, K. W.; Kim, M.; Du Bois, J. *J. Am. Chem. Soc.* **2004**, *126*, 15378–15379. (b) Fiori, K. W.; Du Bois, J. *J. Am. Chem. Soc.* **2007**, *129*, 562–568.

(11) Nörder, A.; Herrmann, P.; Herdtweck, E.; Bach, T. *Org. Lett.* **2010**, *12*, 3690–3692.

(12) *syn-3a*: colorless column, $C_{12}H_{15}BrCl_3NO_4S$, $M_r = 455.57$; monoclinic, space group $P2_1/n$ (No. 14), $a = 11.1241(4)$ Å, $b = 9.1560(3)$ Å, $c = 17.8862(6)$ Å, $\beta = 103.4214(15)^\circ$, $V = 1772.00(11)$ Å³, $Z = 4$, $\lambda(\text{Mo K}\alpha) = 0.71073$ Å, $\mu = 2.904$ mm⁻¹, $\rho_{\text{calcd}} = 1.708$ g cm⁻³, $T = 123(1)$ K, $F(000) = 912$, $\theta_{\text{max}}: 25.38^\circ$, $R1 = 0.0252$ (3126 observed data), $wR2 = 0.0679$ (all 3245 data), $GOF = 1.049$, 205 parameters, $\Delta\rho_{\text{max/min}} = 0.96/-0.56$ e Å⁻³. For more details, see SI. CCDC-868964.

(13) Tellitu, I.; Domínguez, E. *Tetrahedron* **2008**, *64*, 2465–2470.

(14) Höfle, G.; Steglich, W.; Vorbrüggen, H. *Angew. Chem., Int. Ed. Engl.* **1987**, *17*, 569–583.

(15) Mandal, A. N.; Raychaudhuri, S. R.; Chatterjee, A. *Synthesis* **1983**, 727–729.

(16) Zalatan, D. N.; Du Bois, J. *J. Am. Chem. Soc.* **2009**, *131*, 7558–7559.

(17) (a) Reddy, R. P.; Davies, H. M. L. *Org. Lett.* **2006**, *8*, 5013–5016. (b) Mayer, A. C. *Synthesis* **2008**, 945–946.

(18) Davies, H. M. L.; Dick, A. R. *Top. Curr. Chem.* **2010**, *292*, 303–345.

(19) For a DFT study on the Rh-catalyzed C–H bond activation/C–C bond formation with diazo compounds, see: Nakamura, E.; Yoshikai, N.; Yamanaka, M. *J. Am. Chem. Soc.* **2002**, *124*, 7181–7192.

(20) (a) Au, S.-M.; Huang, J.-S.; Yu, W.-Y.; Fung, W.-H.; Che, C.-M. *J. Am. Chem. Soc.* **1999**, *121*, 9120–9132. (b) See also: Nägeli, I.; Bernardinelli, G.; Jacquier, Y.; Moran, M.; Müller, P. *Helv. Chim. Acta* **1997**, *80*, 1087–1105.

(21) (a) Streitwieser, A., Jr.; Jagow, R. H.; Fahery, R. C.; Suzuki, S. *J. Am. Chem. Soc.* **1958**, *80*, 2326–2332. (b) DeFrees, D. J.; Hehre, W. J.; Sunko, D. E. *J. Am. Chem. Soc.* **1979**, *101*, 2323–2327. (c) Amaoudrat, J.; Wiest, O. *J. Am. Chem. Soc.* **2000**, *122*, 3367–3374.

(22) Lin, X.; Zhao, C.; Che, C.-M.; Ke, Z.; Philipps, D. L. *Chem. — Asian J.* **2007**, *2*, 1101–1108.

(23) (a) Espino, C. G.; Du Bois, J. *Angew. Chem., Int. Ed.* **2001**, *40*, 598–600. (b) Fiori, K. W.; Espino, C. G.; Brodsky, B. H.; Du Bois, J. *Tetrahedron* **2009**, *65*, 3042–3051.

(24) (a) Becke, A. D. *Phys. Rev. A* **1988**, *38*, 3098. (b) Perdew, J. P.; Burke, K.; Wang, Y. *Phys. Rev. B* **1996**, *54*, 16533.

(25) Hay, P. J.; Wadt, W. R. *J. Chem. Phys.* **1985**, *82*, 299.

(26) For current mechanistic work, see: Kornecki, K. P.; Berry, J. F. *Chem.—Eur. J.* **2011**, *17*, 5872–5832.

(27) Legault, C. Y. *CYLview*, 1.0b; Université de Sherbrooke:Sherbrooke, Quebec, Canada, 2009; <http://www.cylview.org>.

(28) Reed, A. E.; Weinstock, R. B.; Weinhold, F. *J. Chem. Phys.* **1985**, *83*, 735.

(29) Leaving a tunnel effect apart, theory predicts a maximum primary deuterium KIE of $k_H/k_D = 7.0$ at 300 K for a scenario, in which the stretching vibration of A and B in a linear transition state $A\cdots H(D)\cdots B$ is symmetrical. For a theoretical treatise, see: Westheimer, F. *Chem. Rev.* **1961**, *61*, 265–273.

(30) *trans-10d*: colorless fragment, $C_{14}H_{15}Cl_3N_2O_4S$, $M_r = 413.70$; orthorhombic, space group $Pca2_1$ (No. 29), $a = 18.4231(5)$ Å, $b = 9.1321(3)$ Å, $c = 10.0716(3)$ Å, $V = 1694.46(9)$ Å³, $Z = 4$, $\lambda(\text{Mo K}\alpha) = 0.71073$ Å, $\mu = 0.686$ mm⁻¹, $\rho_{\text{calcd}} = 1.622$ g cm⁻³, $T = 123(1)$ K, $F(000) = 848$, $\theta_{\text{max}}: 25.37^\circ$, $R1 = 0.0154$ (3086 observed data), $wR2 = 0.0412$ (all 3095 data), $GOF = 1.073$, 278 parameters, $\Delta\rho_{\text{max/min}} = 0.17/-0.22$ e Å⁻³. For more details, see SI. CCDC-868965.

(31) (a) Wei, J.-F.; Zhang, L.-H.; Chen, Z.-G.; Shi, X.-Y.; Cao, J.-J. *Org. Biomol. Chem.* **2009**, *7*, 3280–3284. (b) Chen, Z.-G.; Wei, J.-F.; Wang, M.-Z.; Zhou, L.-Y.; Zhang, C.-J.; Shi, X.-Y. *Adv. Synth. Catal.* **2009**, *351*, 2358–2368. (c) Thakur, V. V.; Talluri, S. K.; Sudalai, A. *Org. Lett.* **2003**, *5*, 861–864.

(32) *trans-11c*: colorless needle, $C_{15}H_{18}Cl_3NO_6S$, $M_r = 446.72$; triclinic, space group $P\bar{1}$ (No. 2), $a = 6.0092(2)$ Å, $b = 10.8340(3)$ Å, $c = 14.5195(4)$ Å, $\alpha = 88.5906(14)^\circ$, $\beta = 78.7501(11)^\circ$, $\gamma = 80.8585(12)^\circ$, $V = 915.32(5)$ Å³, $Z = 2$, $\lambda(\text{Mo K}\alpha) = 0.71073$ Å, $\mu = 0.648$ mm⁻¹, $\rho_{\text{calcd}} = 1.621$ g cm⁻³, $T = 173(1)$ K, $F(000) = 460$, $\theta_{\text{max}}: 25.44^\circ$, $R1 = 0.0268$ (3060 observed data), $wR2 = 0.0725$ (all

3377 data), $GOF = 1.020$, 307 parameters, $\Delta\rho_{\text{max/min}} = 0.54/-0.45$ e Å⁻³. For more details see SI. CCDC-868966.

(33) *trans-11d*: colorless fragment, $C_{14}H_{15}Cl_3N_2O_4S$, $M_r = 413.70$; monoclinic, space group $P2_1/c$ (No. 14), $a = 10.2165(3)$ Å, $b = 18.2740(6)$ Å, $c = 10.1200(3)$ Å, $\beta = 111.3324(12)^\circ$, $V = 1759.92(9)$ Å³, $Z = 4$, $\lambda(\text{Mo K}\alpha) = 0.71073$ Å, $\mu = 0.660$ mm⁻¹, $\rho_{\text{calcd}} = 1.561$ g cm⁻³, $T = 123(1)$ K, $F(000) = 848$, $\theta_{\text{max}}: 25.40^\circ$, $R1 = 0.0254$ (3078 observed data), $wR2 = 0.0702$ (all 3221 data), $GOF = 1.076$, 277 parameters, $\Delta\rho_{\text{max/min}} = 0.42/-0.38$ e Å⁻³. CCDC-868967. For more details see SI.